JOURNAL OF PROPULSION AND POWER
Vol. 25, No. 2, March–April 2009

Experimental Verification for Acoustic Damping Enhancement by Gaps in Injector-Formed Baffles

K. J. Lee,* H. J. Kim,† S. Seo,* and H. S. Choi‡
Korea Aerospace Research Institute, Daejeon 305-333, Republic of Korea

DOI: 10.2514/1.40589

The effect of baffle gaps on the damping enhancement of a liquid rocket engine combustor has been elucidated through a series of tests, which include cold acoustic tests under both atmospheric and simulated viscous conditions and simulated combustion tests. The injector-formed baffles, which consist of an array of protruded coaxial injectors, were found to have a much greater acoustic damping effect than conventional planar baffles. For several axial baffle lengths, an optimal acoustic damping capacitance has been achieved at a 0.1 ∼ 0.2 mm baffle gap. The reason there exists an optimal baffle gap is thought to be mainly due to the viscous dissipation at the surface of the injector-formed baffles. Consequently, the axial baffle length can be reduced by taking advantage of the optimal baffle gap, providing a possible solution to the thermal cooling problem persistent with the baffle. Moreover, these optimum characteristics can provide some guidelines for manufacturing and assembling of the baffled injectors in rocket combustors.

Nomenclature

c	=	sonic velocity
D_{ch}	=	diameter of chamber
f	=	frequency
K_m	=	mixture ratio
L_B	=	axial baffle length
L_{ch}	=	axial length of chamber
p_{ch}	=	chamber pressure
R	=	combustion stability margin
R_{ch}	=	radius of chamber
α_{mn}	=	transversal eigenvalue
Δ	=	gap between baffled injectors or injector-formed baffles
η	=	damping factor
μ	=	viscosity
ν	=	kinematic viscosity
ρ	=	density

Subscripts

a	=	nominal operation condition of the actual combustor
B	=	baffle
ch	=	chamber
m	=	index representing radial acoustic modes
n	=	index representing tangential acoustic modes
q	=	index representing axial acoustic modes
UB	=	unbaffled case

I. Introduction

THERE are two conflicting concerns in the development of new rocket engine combustors, which include performance and stability. Generally, combustors of high performance have many opportunities to encounter combustion instabilities [1,2]. High-frequency combustion instabilities, also known as acoustic instabilities, have been induced by the in-phase interaction of an acoustic field and combustion responses. These undesirable phenomena can cause deterioration of propulsion performance and even cause severe physical damage on the injector faceplate and the chamber wall in power-generating devices such as ramjets, turbojet thrust augmentors, utility boilers, industrial furnaces, and especially rocket combustors [1–7].

In attempts to eliminate these instability problems, the modifications and additions of engine components can be used for both passive and active control. As passive control methods, baffles and acoustic cavities, which modify the acoustic fields of a combustion chamber, are frequently used [1–5,8,9]. Baffles can be easily designed in a wide variety of shapes and can be applied to relatively more acoustic modes than acoustic cavities, and, therefore, baffles can overcome the narrow band characteristic of acoustic cavities. However, accompanying problems, such as cooling and structural integrity, would be severe at high pressure due to the increased thermal load to the baffle surfaces. To minimize these cooling and performance/thrust-loss problems with installed baffles, a shortening or lengthening optimization process [10] is necessary to satisfy both damping capacity and thermal survivability.

Mechanisms of combustion instability in liquid rocket combustors are very complex, involving many processes such as injection, atomization, vaporization, mixing, and chemical reactions. Although a number of works on this issue have been studied [1,2,4–6,8], only limited information is available to predict and suppress combustion instabilities. Ideally, experimental approaches using full-scale combustion chambers with actual injectors [5,8,10] would be the most reliable methods, but these are very expensive and time consuming. To overcome these cost and time problems, it is necessary to find some simple, cost-effective method without neglecting the essential performance characteristics. In this respect, subscale test methodology [4,11–17] has been applied recently and widely used to evaluate combustion stability. The main assumption of this methodology is that the mixing process is dominant, leading to high-frequency combustion instabilities. Dranovsky [4] and Fisher et al. [11] have summarized these experimental techniques and discussed the advantages and the limitations of using combustors of various scales.

When coaxial injectors are adopted in a full-scale combustor, baffles formed by injectors protruding from the faceplate, referred to as injector-formed baffles or baffled injectors, would be recommended [4,9,18]. In this case, some gap or mechanical clearance between injectors that form the baffles is thought to be inevitable. Sutton [18] has just mentioned that these gaps cause extra damping to an oscillating flow. But any further quantified evaluations on this extra damping effect by these gaps were not

Partially presented as Paper 4446 at the 41st AIAA/ASME/SAE/ASEE Joint Propulsion Conference and Exhibit, Tucson, AZ, 10–13 July 2005; received 26 August 2008; revision received 18 November 2008; accepted for publication 30 November 2008. Copyright © 2008 by the American Institute of Aeronautics and Astronautics, Inc. All rights reserved. Copies of this paper may be made for personal or internal use, on condition that the copier pay the $10.00 per-copy fee to the Copyright Clearance Center, Inc., 222 Rosewood Drive, Danvers, MA 01923; include the code 0748-4658/09 $10.00 in correspondence with the CCC.

*Senior Researcher, Combustion Chamber Department.
†Senior Researcher, Combustion Chamber Department; khongjip@kari.re.kr (Corresponding Author).
‡Head, Combustion Chamber Department.

given. In the present study, the effect of gaps on acoustic damping characteristics has been investigated acoustically as a preliminary step. A damping factor has been selected to quantify the acoustic damping capability in cold acoustic tests. Furthermore, through the previously mentioned subscale combustion tests, which can couple the injection dynamics and chamber acoustics, the stability margins are evaluated as a function of the gaps between the protruded injectors to scrutinize the optimal gap for high damping capacity. From these nonreacting acoustic tests and reacting hot-firing tests, the enhanced damping effect of these gaps has been verified. Consequent results from acoustic and hot-firing tests could be used to create a database to provide guidelines for the manufacturing and assembling of injector-formed baffles.

II. Cold Acoustic Tests

A. Experimental Methods

As shown in Fig. 1, an atmospheric cold acoustic experimental setup as a first step for the investigation of acoustic damping enhancement caused by gaps between baffled injectors consists of a random signal generator, microphones for sensing (B&K 4190), a data acquisition system (B&K PULSE 3560D), and a model chamber. Random signals are introduced via a loudspeaker, which has been installed in the periphery of the faceplate. Three microphones, each of which has been located 50 mm radially, are rotated in every 20 deg transversely and swept axially to determine the acoustic modes in the model chamber. One reference microphone has been installed in the faceplate to characterize acoustic damping capacity.

The model chamber is made of stainless steel and has cylindrical shape of 380 mm in diameter and 475 mm in length. This diameter is the same as the object full-scale combustor to achieve the same resonant frequency of the first tangential (1T) acoustic mode. The aluminum faceplate is 20 mm thick and attached to the model chamber with a rubber O-ring and vacuum grease.

Figure 2 shows the simulated faceplate with baffles of a hub and six blades in the present study. Baffled injectors have been installed to simulate configurations having several gaps such as $\Delta = 0.0, 0.1,$ 0.2, 0.3, 0.4, 0.6, and 1.0 mm. The gaps were measured with a gap gauge and then averaged after installation. Axial baffle lengths have been selected as $L_B = 30$, 50, and 70 mm. When the full-scale combustor is 380 mm in diameter, these values would correspond to about 8, 13, and 18% of the chamber diameter, respectively. All the data have been analyzed with a frequency resolution of 0.125 Hz. In addition, all the acoustic tests have been performed under constant-temperature and constant-humidity conditions.

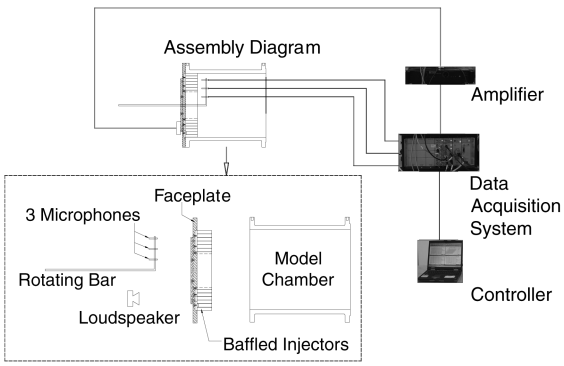

Fig. 1 Experimental setup for cold acoustic tests.

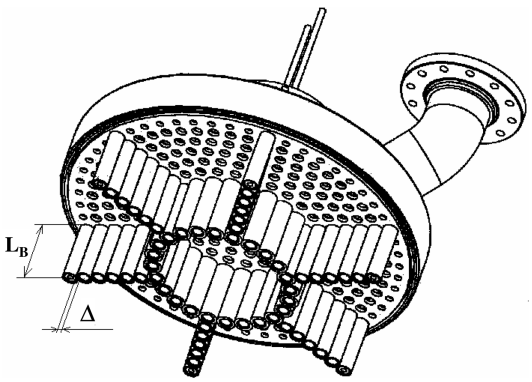

Fig. 2 Schematic of a faceplate with injector-formed baffles.

Among the convenient ways to determine the amount of damping capacity in a system, the measurement of the decay rate of the oscillating pressure and the bandwidth method are widely used [1–3,7,19]. In the present study, acoustic damping capacity has been quantified by a parameter of damping factor η, which is evaluated by bandwidth method

$$\eta = \frac{f_2 - f_1}{f_{\text{peak}}} \tag{1}$$

where f_{peak} is the frequency at which the peak pressure appears and f_1 and f_2 are the frequencies corresponding to $1/\sqrt{2}$ times the peak pressure amplitude with $f_2 > f_1$. Damping factor ratio is defined as η/η_{UB} where η_{UB} is the damping factor of the unbaffled case.

B. Atmospheric Acoustic Tests

First, cold acoustic characteristics of the unbaffled chamber were studied as a preliminary step. In the case of a simple closed cylindrical chamber configuration, the analytic solution for the conventional wave equation is given, and the resonant frequencies can be expressed as follows [7,20]:

$$f_{m,n,q} = \frac{c}{2}\sqrt{\left(\frac{\alpha_{mn}}{R_{\text{ch}}}\right)^2 + \left(\frac{q}{L_{\text{ch}}}\right)^2} \tag{2}$$

where c is the sonic velocity and R_{ch} and L_{ch} are the radius and axial length of the model chamber, respectively. α_{mn} is the transversal eigenvalue and subscripts such as m, n, and q are indices representing radial, tangential, and axial acoustic modes, respectively [7,20].

Compared with analytic resonant frequencies, satisfactory agreement has been achieved from the viewpoint of resonant frequencies, as shown in Table 1. Therefore, the validation of the present measuring data acquisition system and the feasibility of the present test facility for the acoustic estimation of the optimal gap between baffled injectors are well supported.

When the baffled injectors are installed in the faceplate, the baffle hub and blades form some regular embossed configuration with respect to the tangential acoustic flow. Under this condition, broader bandwidth, in other words, a higher damping capacity could be achieved compared with conventional planar baffles. For example, when a 70-mm-long baffle of planar configuration was installed, the damping factor with respect to the unbaffled value, damping factor ratio (DFR), was 1.73. In the case where baffled injectors with the same length were installed in the same model chamber, the DFR was 2.90, about 70% higher than the previous value (1.73). Although ideal installation without any gap could not be achieved in baffled injectors (on average a 0.015 mm gap was measured by the gap gauge), this damping enhancement can be thought to be mainly due to the irregular acoustic reflection and broad acoustic dissipation by the embossed surface of the baffled injectors. Consequently, injector-formed baffles had some advantages over the typical planar baffles in acoustic damping capability.

Table 1 Resonant frequencies of acoustic modes in unbaffled chamber under atmospheric cold condition

Mode	1L	1T	1T1L	2L
Analytic, Hz	357.9	524.3	634.8	715.8
Experiment, Hz	359.9	533.4	643.0	719.6
Error, %	0.56	1.74	1.29	0.53

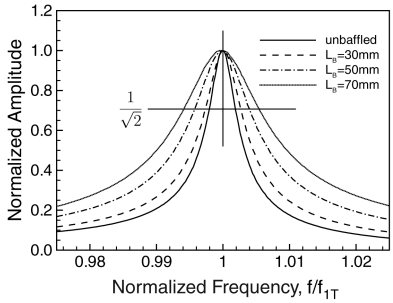

Fig. 3 Damping factor characteristics of the first-tangential mode.

The effect of axial baffle length on acoustic damping characteristics has been analyzed and shown in Fig. 3. The 1T acoustic mode has been selected because this mode is known to be one of the most harmful modes in practical combustion chambers of liquid rocket engines. The acoustic path of transverse modes increases with axial baffle length, and so does the broadness of the acoustic responses. Therefore, the resonant frequency of this mode decreases monotonically. Moreover, acoustic damping increases with axial baffle length. This phenomenon is qualitatively the same as the previous experimental and numerical results [7,19,21]. For a careful determination of the axial baffle length in actual full-scale combustors, other considerations, such as thermal cooling and structural problems, should be included in addition to acoustic damping characteristics.

Next, the effect of gap size between baffled injectors under $L_B =$ 70 mm has also been investigated. Figure 4 shows cold acoustic responses of 1T mode with respect to the various baffle gaps. The peak amplitude of the 1T mode decreases while its bandwidth or DFR increases drastically in the vicinity of $0.1 \sim 0.2$ mm gap range. On the other hand, the resonant frequency increases with the gap because the acoustic field cannot be confined by the baffle gap. However, when the gap was larger than 0.2 mm, the peak amplitude and the resonant frequency of the 1T mode increased gradually and finally asymptotically approach the unbaffled condition (533.4 Hz).

The behavior of the resonant frequency and the damping factor ratio are shown in Fig. 5. There exists a certain optimum value of the gaps between the baffled injectors at which relatively high damping characteristics can be attained. From the characteristics of the damping factor ratio, higher damping capacity at the same axial baffle length can be obtained if a certain value of gap can be managed, for example $0 \sim 0.8$ mm in this 70 mm baffle case, as shown in Fig. 5.

Acoustic sound power, shown in Fig. 6, has also been investigated to elucidate the high damping capacity at the optimal gap. Acoustic sound power level (SPL) is proportional to the square of acoustic pressure amplitude [20]. In the present study, this intensity was evaluated by integrating the square of the pressure amplitude over the frequency domain $\mathrm{SPL} \sim \int p'^2 \mathrm{d}f$. The frequency range was determined at the negligible amplitude compared with the resonant amplitude, which can be expected from the similar figure like Fig. 3.

In the cases of high damping capacitance (0.1 and 0.2 mm in Fig. 6), acoustic sound power is lower than the other cases. This phenomenon can be thought to indicate that some energy dissipation mechanisms occur at a $0.1 \sim 0.2$ mm gap such as acoustic absorption and viscous dissipation at the embossed surface of the array of the baffled injectors. Previously, this additional damping effect by the gaps has been simply mentioned by Sutton [18]. In the present study, further systematic investigation of the acoustic enhancement by the gaps will be discussed in the following sections.

Overall acoustic characteristics are shown in Fig. 7. As expected, the shorter the baffle is, the closer the frequency becomes to the resonant frequency of the unbaffled case and the less the damping is for a given injector gap. Especially in the case of $L_B = 30$ mm ($L_B/D_{\mathrm{ch}} \approx 8\%$), the frequency shift is not relatively dominant compared with the other cases. As shown in Fig. 7b, higher damping

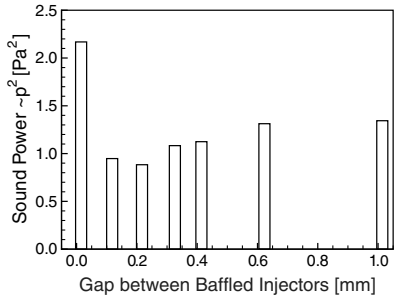

Fig. 6 Variations of acoustic sound power of 70 mm baffled chamber.

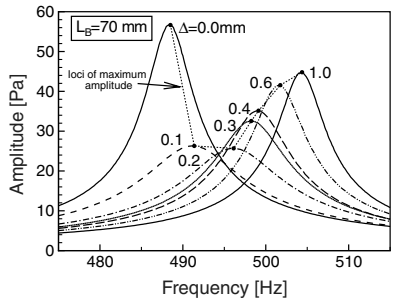

Fig. 4 Frequency response characteristics of 70 mm baffled chamber.

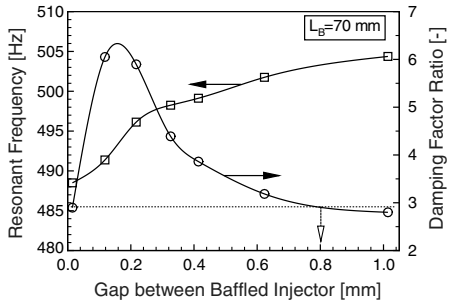

Fig. 5 Variations of resonant frequencies and damping factor ratios of 70 mm baffled chamber.

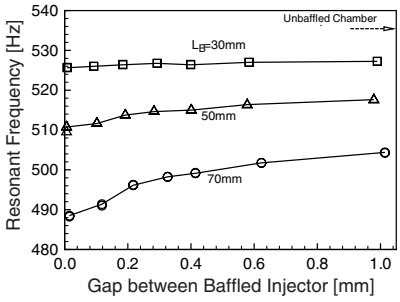

a) Resonant frequency

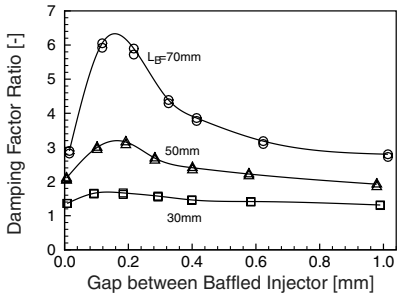

b) Damping factor ratio

Fig. 7 Variations of resonant frequency and damping factor ratio for axial baffle lengths and gaps.

capacity at a shorter axial baffle length can be attained if the gap of baffled injectors is optimally adjusted. For example, 50 mm baffled injectors with $0.1 \sim 0.2$ mm gaps can generate similar or higher levels of acoustic damping than 70 mm baffles without any gap. In reality, this tendency cannot be a sufficient condition on whether combustion stabilization would be obtained in the actual firing condition.

C. Cold Acoustic Tests for Viscous Effects

Previously, we obtained acoustic damping enhancement by baffle gap in atmospheric cold acoustic tests. The main mechanism is thought to be due to viscous dissipation. As a next step, it is necessary to scrutinize this reasoning. To elucidate the viscous effect on acoustic damping, acoustic tests have been done for various viscous conditions. In the case of a combustor having a nominal chamber pressure of 5.25 MPa and a mixture ratio of 2.44, the temperature near the surface of the baffled injectors can be assumed to be $600 \sim 800$ K through regenerative cooling in the baffled injectors. The viscous coefficient under this condition can be evaluated through equilibrium analysis [22]. Although the nonequilibrium condition prevails in this low-temperature regime, qualitative comparison is possible through this equilibrium assumption. The rectangular symbols in Fig. 8 show these viscous coefficient values by equilibrium analysis under a chamber pressure of 5.25 MPa and a mixture ratio of 2.44.

In the case of acoustic tests without combustion, it would be convenient to simulate viscous conditions by changing the pressure instead of changing the temperature of the model combustors. The circular symbols in Fig. 8 show this tendency with respect to simulating pressure. According to this simulation rule, the viscosity of the combustion products under a nominal chamber pressure of 5.25 MPa and a temperature of 1500 K near the baffle can be simulated by air at room temperature under a pressure of about 2.2 bar. Therefore, actual viscous variations in simulated acoustic tests were accomplished by changing the pressure in the simulated combustor. Pressure is changed by using compressed air.

Generally, imposed acoustic intensity is known to be proportional to the density (ρ) and sonic velocity (c) of the medium [20]. Also the absolute quantity of energy dissipated by viscous effects is proportional to the viscous coefficient (μ). To quantify the dissipated energy with respect to the imposed acoustic energy, kinematic viscosity defined as $\nu = \mu/\rho$ should be used. Consequently, this simulation procedure, as shown in Fig. 8, has been applied in the present study.

By changing the pressure in a model simulation chamber, several acoustic tests were performed to study the acoustic characteristics with respect to the viscosity. The results are shown in Fig. 9a. Without gaps between baffled injectors ($\Delta = 0.0$ mm), there is no significant change with respect to pressure. On the contrary, the damping capacity increases markedly with the pressure when a baffle gap exists, especially between 0.1 and 0.2 mm. Also, when the gap was 0.1 mm, a remarkable increase in the damping factor was observed. This tendency can be easily shown by expressing the damping factor in terms of fluid viscosity. Figure 9b shows the variations of damping factors with respect to the viscosity of air in the simulation chamber. As shown in Fig. 9b, the damping capacity increases with the kinematic viscosity of air for all gaps between baffled injectors. Especially when the gaps are in the range of $0.1 \sim 0.2$ mm, a remarkable increase in the damping factor with respect to the viscosity has been observed. Likewise, a marked decrease in the damping factor with respect to the chamber pressure is seen in the same baffle-gap range. Therefore, the effects of viscosity on acoustic damping capacity could be thought tentatively to be dominant.

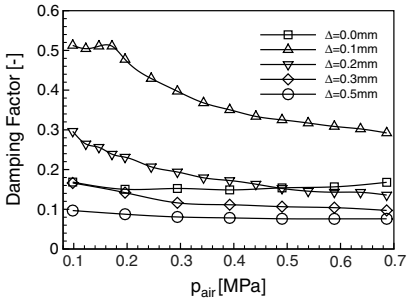

a) Damping factors for various pressures in the model chamber

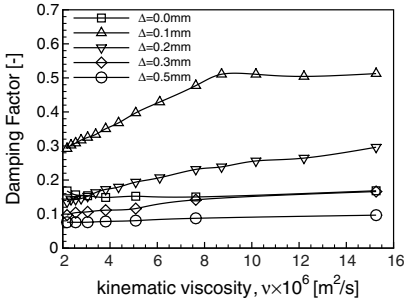

b) Damping factors for kinematic viscosity in the model chamber

Fig. 9 Variations of damping factors for various baffle gaps in terms of pressure and kinematic viscosity.

For a better understanding, the damping capacity for various baffle gaps has been plotted in Fig. 10. This figure shows qualitatively the same behavior as Fig. 7 from the atmospheric cold acoustic tests. The results of Figs. 9 and 10 could be thought to verify that one of the main parameters determining the damping enhancement in the optimal gap range is the viscosity of the fluid near the surface of the circular baffled injectors.

As a result, the main reason that the optimal gap has high acoustic damping capacity is the viscous dissipation occurring at the surface of the baffle injectors, which results in the increase of the dissipation and absorption of acoustic energy. Also, an abrupt acoustic pressure gradient exists at relatively narrow gap regions, causing vortex formation at this surface. Consequently the amplitude of acoustic pressure oscillations decreased at a certain range of gap ($0.1 \sim 0.2$ mm). For a further increase in baffle gap, above 0.2 mm, acoustic waves can propagate through the gap, and the

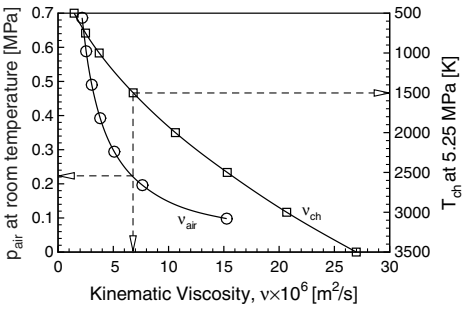

Fig. 8 Variations of kinematic viscosity of kerosene–oxygen combustion product and air at room temperature in a model chamber.

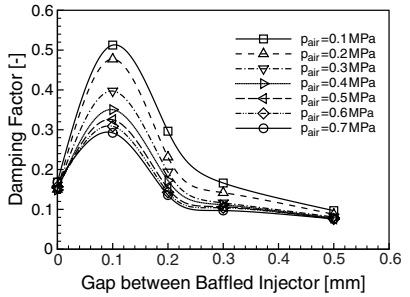

Fig. 10 Variations of damping factors for various gaps between baffled injectors in the model chamber.

viscous effect becomes of little importance, resulting in the decrease of acoustic damping.

III. Simulated Combustion Tests for Feasible Verification

As a verification step, simulated combustion tests have been done. Following are the detailed descriptions of these combustion tests.

A. Subscale Single-Element Test Facility for Firing Tests

The main injectors employed in full-scale combustors are liquid–liquid double swirl coaxial injectors, and the actual propellants are kerosene and liquid oxygen. As mentioned earlier, the nominal chamber pressure p_{ch} and the mixture ratio K_m are 5.25 MPa and 2.44, respectively. Schematic diagrams of this injector having a 1.9 mm recess length and the model chamber are shown in Fig. 11. The subscale model chamber has a cylindrical shape. To maintain the chamber acoustics, the geometric dimensions of the subscale chamber should be chosen to provide the same resonant frequencies in the subscale chamber as those in the full-scale chamber. The detailed method and procedure of selecting the geometric dimensions of the subscale model chamber have been described in previous works [4,12–15,17]. The determined dimensions of the subscale chamber are 130 mm in diameter and 280 mm in axial length. Therefore, the resulting resonant frequencies of the two principal transverse acoustic modes, 1T and 1T1L (the combined acoustic mode of the first tangential and the first longitudinal modes) are estimated analytically to be $f_{1T} \approx 1900$ Hz and $f_{1T1L} \approx 1930$ Hz. This model chamber operates at atmospheric pressure with the upward exit open. Therefore, the 1T1L mode becomes dominant while the 1T mode vanishes. Because of this reason, the stability of 1T1L mode has been investigated.

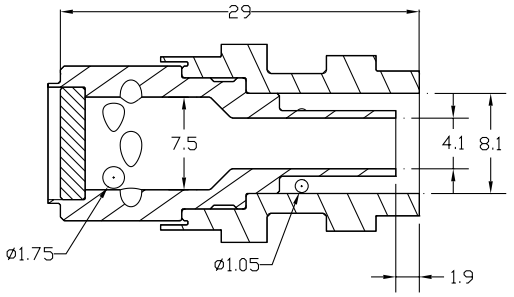

a) An injector

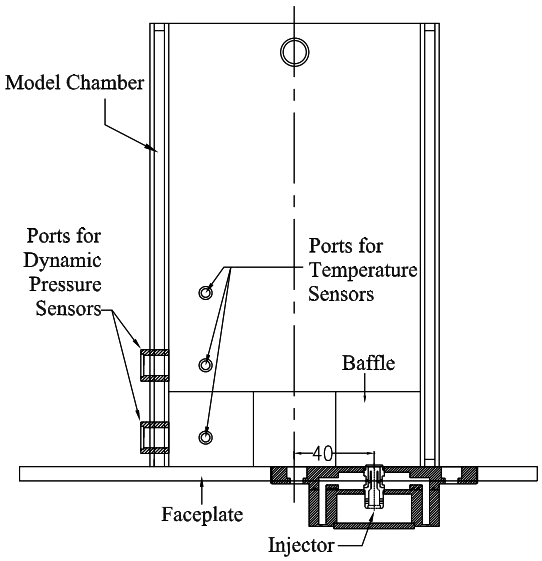

b) A model chamber

Fig. 11 Schematic of the injector element and the model chamber in the present study.

A single-element injector unit is mounted on the faceplate. The injector was installed near the peripheral boundary to be able to simulate the transverse acoustic modes, as shown in Fig. 11b. The model chamber has two sensor ports for pressure, three ports for temperature (for the accurate estimation of sonic velocity), and a water-cooled jacket to prevent overheating of the model chamber.

A schematic diagram of the subscale firing test setup is shown in Fig. 12. The mass flow rates of the propellants are controlled with a throttling device connected to a PC receiving signals from the pressure and temperature sensors upstream of the orifices. The present measurement system can measure mass flow rates with an accuracy of 2%. To measure propellant temperature directly upstream of the injector, thermocouples are installed in the oxidizer and fuel manifolds. The signals from the pressure transducers are amplified by a broadband amplifier, recorded by a PC, and sent to visual instruments (i.e., an oscilloscope, a digital voltmeter, and a spectrum analyzer).

B. Extrapolation of Model-Test Data to Actual Operating Conditions

According to the assumption that the mixing process is the most important mechanism leading to high-frequency combustion instabilities, the oxidizer and fuel have been simulated by gaseous oxygen and gaseous methane, respectively, while maintaining the oxidizer-to-fuel density ratio equal to that of the actual full-scale chamber. A scaling-up method to extrapolate the model operating conditions to actual operating conditions is based on the assumption that with model propellant parameters chosen, there must be equal volumetric flow rates of oxidizer and fuel per bipropellant swirl injector installed in the model or actual combustion chambers (i.e., $Q_{f,a} = Q_{f,m} = 0.135$ l/s and $Q_{o,a} = Q_{o,m} = 0.207$ l/s). More explanations can be found in the previous literature [4,12–15,17].

To determine the combustion stability margin, it is useful to use customary coordinates for the convenient presentation of these stability boundaries, for example, the chamber pressure p_{ch} vs the mixture ratio K_m. First, with the correlation of mixture ratio and characteristic velocity C^* [23], the chamber pressure p_{ch} can be determined through $p_{\mathrm{ch}} = \dot{m}_{\mathrm{tot}} \cdot C^*/A_{\mathrm{th}}$, where $\dot{m}_{\mathrm{tot}}$ is total mass flow rate and A_{th} is the nozzle throat area.

The evaluation of the high-frequency combustion instability is made instantaneously during the test based on the characteristics of pressure oscillations and the spectral behavior of these oscillations. Combustion processes resulting in irregular acoustic oscillations with a broadband spectrum are considered to be stable. Combustion processes that exhibit regular oscillatory behavior, almost sinusoidal in nature, with a spectrum containing individual sharp peaks are considered to be unstable. Unstable regimes are classified into small

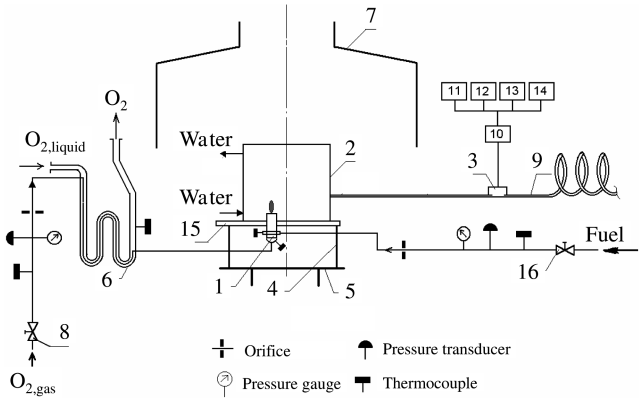

Fig. 12 Experimental schematic for the simulating combustion tests using gaseous propellants showing 1 injector, 2 model chamber, 3 pressure pulsations transducer, 4 support, 5 table, 6 oxidizer heat exchanger, 7 exhaust vent, 8 throttle, 9 acoustic probe, 10 broadband amplifier, 11 oscilloscope, 12 spectrum analyzer, 13 digital voltmeter, 14 PC, 15 injector faceplate, and 16 propane line throttle.

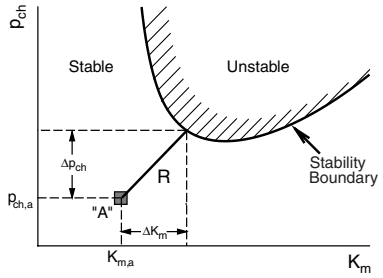

Fig. 13 Conceptual diagram of determining combustion stability margin, R.

amplitude (SA) and large amplitude (LA) oscillations. As a rule, the amplitude of SA oscillations is about $3 \sim 4$ times higher than the noise level, whereas the amplitude of LA oscillations is more than 10 times the noise level. The detailed procedure can be found in the literature [4,12–15,17].

The stability boundary can be plotted in the p_{ch}-K_m coordinate plane, as shown in Fig. 13. Point A denotes the nominal operation condition of the actual combustion chamber. R denotes the minimum distance from the nominal condition (point A) to the stability boundary. The stability margin can quantify how far the unstable region is located from the nominal operating condition and is defined in nondimensional form as [4,12–15,17]

$$R = \sqrt{\left(\frac{\Delta p_{\mathrm{ch}}}{p_{\mathrm{ch},a}}\right)^2 + \left(\frac{\Delta K_m}{K_{m,a}}\right)^2} \tag{3}$$

where $\Delta p_{\mathrm{ch}} = p_{\mathrm{ch}} - p_{\mathrm{ch},a}$ and $\Delta K_m = K_m - K_{m,a}$.

C. Effects of Baffle Gaps

For a baffle length of 50 mm, which was confirmed experimentally to be long enough to stabilize combustion passively through several hot-firing tests [24], damping characteristics for various baffle gaps (0.0, 0.1, 0.2, 0.3, and 0.5 mm) have been studied to scrutinize and verify the effects of baffle gaps on damping enhancement.

Unstable regions in terms of chamber pressure and mixture ratio are shown in Fig. 14. Spontaneous instability regions induced by the 1T1L mode in the simulating chamber existed in cases where the baffle gaps were 0.0, 0.3, and 0.5 mm. On the contrary, unstable regions did not exist with baffle gaps of 0.1 and 0.2 mm, showing very small amplitude of pressure oscillations compared with other cases. Above these stability boundaries, direct flame extinction was observed without showing any unstable responses.

The resonant frequency of the 1T1L mode increased with baffle gap, which is shown in Fig. 15. This tendency is qualitatively the same as that of the cold acoustic tests. The resonant frequency increased with the baffle gap and finally asymptotically approached that of 1T in the unbaffled full-scale chamber (1930 Hz).

The damping response characteristics have been expressed in terms of the combustion stability margin and shown in Fig. 16. The combustion stability margin had a maximum value near the baffle gap of $0.1 \sim 0.2$ mm. These results are qualitatively the same as

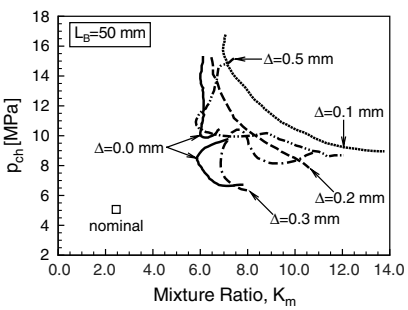

Fig. 14 Instability regions by self-oscillation for various baffle gaps in the model chamber.

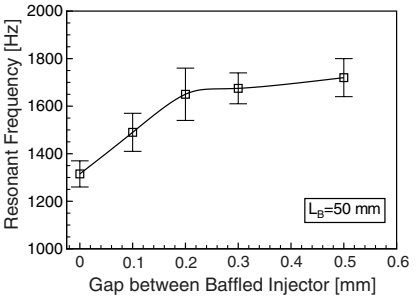

Fig. 15 Variations of resonant frequencies of 1T1L for various baffle gaps in the model chamber.

those of the cold acoustic tests, as were given in the preceding section.

In addition, the amplitude response characteristics are shown in Fig. 17. The maximum amplitudes in Fig. 17 are the amplitudes of self-oscillations near the instability regions corresponding to the stability margin R. Similarly, in a certain optimal range of baffle gap ($0.1 \sim 0.2$ mm), the amplitude decreased dramatically. However, above this optimal range, the amplitude increased with the baffle gap. Generally, the maximum amplitude of pressure oscillations is thought to be inversely proportional to the combustion stability capacity. So the results of Figs. 16 and 17 are assumed to be consistent with each other.

From all the results of the atmospheric cold acoustic tests, viscosity-simulating cold acoustic tests, and these simulated combustion tests, it is probable that the main reason the optimal gap has a high damping capacity is due to the viscous dissipation of acoustic energy at the surface of the circular baffle. This tendency was verified through the combustion tests, in which the coupling of the acoustic field and the combustion field could be obtained. For the better verification of viscous dissipation and vortex formation, studies on flow characteristics using analytical methods [25,26], CFD, or visualization methods are necessary as future works.

Actually, baffles without any gaps are thought to be impossible, thus the resultant baffle gap is inevitable in the viewpoint of practical manufacturing of injectors and assembling them with the faceplate. If the gaps can be controlled within this optimal range, better damping

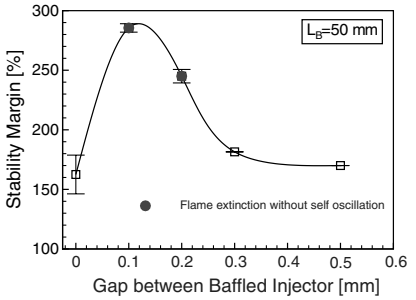

Fig. 16 Combustion stability margins for various baffle gaps under $L_B = 50$ mm.

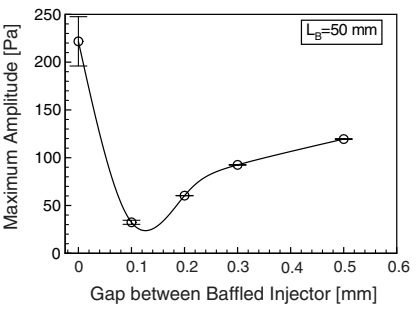

Fig. 17 Variations of maximum amplitude of 1T1L for various baffle gaps in the model chamber.

characteristics can be obtained, which can be inferred from Figs. 7, 10, and 16. Also, shortening of the axial length of the baffled injectors would be probable by using this tendency effectively. In addition, the damping enhancement effect attained by the gaps can mitigate possible thermal cooling problems through the shortening of the axial baffle length. Therefore, the results of the present study can provide effective guidelines for baffle gaps in designing, manufacturing, and assembling combustion chambers.

IV. Conclusions

Baffles can be formed by injectors protruding from the faceplate of a liquid rocket combustor, which can be referred to as injector-formed baffles or baffled injectors. These injector-formed baffles can be used to eliminate high-frequency combustion instabilities when coaxial injectors are mainly used in a liquid rocket combustor. Acoustic damping enhancement by the gaps in the injector-formed baffles has been investigated experimentally. First, the effects of gaps on acoustic damping characteristics of the first tangential mode have been elucidated by atmospheric cold acoustic tests which were done for three different axial baffle lengths and various gaps between these baffled injectors. Injector-formed baffles had much better acoustical damping characteristics than typical planar baffles. Resonant frequency shift with respect to axial baffle lengths shows qualitatively the same results as previous literature. The regular embossed surface of a circular baffle configuration can cause higher damping capacity by random acoustic reflection and viscous dissipation. Irrespective of axial baffle length, an optimal acoustic damping capacity was obtained with a $0.1 \sim 0.2$ mm gap. Next, cold acoustic tests for the elucidation of viscous effects were performed by simulating various viscous conditions. Qualitatively the same results as those of previous atmospheric cold acoustic tests were obtained. Tentatively, the probable reason of the existence of an optimal gap is thought to be due to the fact that the acoustic absorption by viscous dissipation at the baffle surfaces may increase the damping capacity. As a feasible verification step, simulated combustion tests were performed. In terms of the combustion stability margin, satisfactory agreement was obtained with previous nonreacting acoustic tests. Finally, summarizing all response characteristics such as the combustion stability margin, the amplitude of pressure oscillations from simulated combustion tests, and the results from cold acoustic tests, one of the main mechanisms governing the damping characteristics around baffle gaps is thought to be the viscous dissipation at the surface of the circular baffles. Because of this phenomenon of viscous energy dissipation, the acoustic damping capacity is enhanced around the optimal range of baffle gap.

Gaps between injector-formed baffles are unavoidable from a manufacturing clearance and assembling viewpoint. By using the positive effect of these gaps on acoustic damping capability, axial baffle length can be reduced, and this characteristic can help thermal cooling problems that may occur by installing baffles in the combustors at a high pressure and severe temperatures. Also, in designing baffled injectors, it would be very important to guarantee the thermal survivability of these baffled injectors during operation. One authentic solution would be the shortening of the baffle length, and this would be probable through these gap effects. Actually these optimal characteristics can provide guidelines for the manufacturing clearance and assembling of injectors in full-scale rocket engines.

Acknowledgment

This research was supported by the Korean Ministry of Education, Science and Technology.

References

[1] Harrje, D. T., and Reardon, F. H. (eds.), "Liquid Propellant Rocket Combustion Instability," NASA SP-194, 1972.

[2] Natanzon, M. S., *Combustion Instability*, Mashinostroyeniye Publishers, Moscow, 1986.

[3] "Liquid Rocket Engine Combustion Stabilization Devices," NASA SP-8113, 1974.

[4] Dranovsky, M. L., *Combustion Instabilities in Liquid Rocket Engines*, edited by V. Yang, F. E. C. Culick, and D. G. Talley, Vol. 221, Progress in Astronautics and Aeronautics, AIAA, Reston, VA, 2007.

[5] Oefelein, J. C., and Yang, V., "Comprehensive Review of Liquid-Propellant Combustion Instabilities in F-1 Engines," *Journal of Propulsion and Power*, Vol. 9, No. 5, 1993, pp. 657–677. doi:10.2514/3.23674

[6] Agarkov, A. F., Denisov, K. P., Dranovsky, M. L., Zavorohin, I. A., Ivanov, V. N., Pikalov, V. P., and Shibanov, A. A., "Injector Flame Stabilization Effects on Combustion Instability," *Liquid Rocket Engine Combustion Instability*, edited by V. Yang, and W. E. Anderson, Vol. 169, Progress in Astronautics and Aeronautics, AIAA, Washington, D.C., 1995, pp. 281–305.

[7] Laudien, E., Pongratz, R., Pierro, R., and Preclik, D., "Experimental Procedures Aiding the Design of Acoustic Cavities," *Liquid Rocket Engine Combustion Instability*, edited by V. Yang,, and W. E. Anderson, Vol. 169, Progress in Astronautics and Aeronautics, AIAA, Washington D.C., 1995, pp. 377–399.

[8] Lourme, D., "Historical Aspects and Characteristics of Liquid Propellant Combustion Instability," *Combustion Instability in Liquid Rocket Engines*, edited by H. F. R. Schöyer, ESA, The Netherlands, 1993, pp. 1–22.

[9] Sutton, G. P., *History of Liquid Propellant Rocket Engines*, AIAA, Reston, VA, 2005.

[10] Kim, H. J., Seo, S., Lee, K. J., Han, Y. M., Lee, S. Y., and Ko, Y. S., "Stability Rating Tests for the Length-Optimization of Baffles in a Liquid Propellant Combustion Chamber Using a Pulse Gun," *Aerospace Science and Technology*, Vol. 12, No. 3, 2008, pp. 214–222. doi:10.1016/j.ast.2007.06.003

[11] Fisher, S. C., Dodd, F. E., and Jensen, R. J., "Scaling Techniques for Liquid Rocket Combustion Stability Testing," *Liquid Rocket Engine Combustion Instability*, edited by V. Yang, and W. E. Anderson, Vol. 169, Progress in Astronautics and Aeronautics, AIAA, Washington D.C., 1995, pp. 545–564.

[12] Sohn, C. H., Seol, W. S., Shibanov, A. A., and Pikalov, V. P., "On the Method for Hot-Fire Modeling of High-Frequency Combustion Instability in Liquid Rocket Engines," *Journal of Mechanical Science and Technology*, Vol. 18, No. 6, 2004, pp. 1010–1018.doi:10.1007/BF02990873

[13] Dexter, C. E., Fisher, M. F., Hulka, J. R., Denisov, K. P., Shibanov, A. A., and Agarkov, A. F., "Scaling Techniques for Design, Development, and Test," *Liquid Rocket Thrust Chambers: Aspects of Modeling, Analysis, and Design*, edited by V. Yang, M. Habiballah, J. Hulka, and M. Popp, Vol. 200, Progress in Astronautics and Aeronautics, AIAA, Reston, VA, 2004, pp. 553–600.

[14] Lee, K. J., Seo, S., Song, J. Y., Han, Y. M., Choi, H. S., and Seol, W. S., "Combustion Stability Assessment of Double Swirl Coaxial Injectors Using Simulant Propellants," *AIAA/ASME/SAE/ASEE Joint Propulsion Conference*, AIAA Paper 2005-4443, 2005.

[15] Sohn, C. H., Seol, W. S., Shibanov, A. A., and Pikalov, V. P., "Combustion Stability Boundaries of the Subscale Rocket Chamber with Impinging Jet Injectors," *Journal of Propulsion and Power*, Vol. 23, No. 1, 2007, pp. 131–139. doi:10.2514/1.19937

[16] Lubarsky, E., Hadjipanayis, M., Shcherbik, D., Bibik, O., and Zinn, B. T., "Control of Tangential Instability by Asymmetric Baffle," *46th AIAA Aerospace Sciences Meeting and Exhibit*, AIAA Paper 2008-955, 2008.

[17] Cavitt, R. C., Frederick, R. A., Jr., and Bazarov, V. G., "Laboratory Scale Survey of Pentad Injector Stability Characteristics," *Journal of Propulsion and Power*, Vol. 24, No. 3, 2008, pp. 534–540. doi:10.2514/1.32618

[18] Sutton, G. P., "History of Liquid-Propellant Rocket Engines in Russia, Formerly the Soviet Union," *Journal of Propulsion and Power*, Vol. 19, No. 6, 2003, pp. 1008–1037. doi:10.2514/2.6943

[19] Kim, S.-K., Kim, H. J., Seol, W. S., and Sohn, C. H., "Acoustic Stability Analysis of Liquid Propellant Rocket Combustion Chambers," *AIAA/ASME/SAE/ASEE Joint Propulsion Conference*, AIAA Paper 2004-4142, 2004.

[20] Zucrow, M. J., and Hoffmann, J. D., *Gas Dynamics*, Vol. 2, Wiley, New York, 1977.

[21] Wicker, J. M., Yoon, M. W., and Yang, V., "Linear and Non-linear Pressure Oscillations in Baffled Combustion Chambers," *Journal of Sound and Vibration*, Vol. 184, 1995, pp. 141–171. doi:10.1006/jsvi.1995.0309

[22] McBride, B. J., and Gordon, S., "Computer Program for Calculation of Complex Chemical Equilibrium Compositions and Applications," NASA Reference Publication 1311, 1996.

[23] Sutton, G. P., *Rocket Propulsion Elements*, 6th ed., Wiley, New York, 1992.

[24] Lim, B., Lee, K. J., Kim, J. K., Ahn, K., Kim, H. J., Seo, S., and Choi, H. S., "Stability Rating Tests of 30 ton Class Regeneratively Cooled Combustor," *Proceedings of the 2008 Korean Society for Aeronautical and Space Sciences Spring Conference*, 2008, pp. 826–829.

[25] Eldredge, J. D., and Dowling, A. P., "The Absorption of Axial Acoustic Waves by a Perforated Liner with Bias Flow," *Journal of Fluid Mechanics*, Vol. 485, 2003, pp. 307–335. doi:10.1017/S0022112003004518

[26] Eldredge, J. D., "On the Interaction of Higher Duct Modes with a Perforated Liner System with Bias Flow," *Journal of Fluid Mechanics*, Vol. 510, 2004, pp. 303–331. doi:10.1017/S0022112004009504

D. Talley
Associate Editor